# Photoinduced valley currents in strained graphene

T. L. Linnik*

*Department of Theoretical Physics, V. E. Lashkaryov Institute of Semiconductor Physics, National Academy of Sciences of Ukraine, 03028 Kyiv, Ukraine*

(Received 5 June 2014; revised manuscript received 19 July 2014; published 7 August 2014)

The theoretical results are presented showing that strain-induced anisotropy of graphene spectrum gives rise to the valley currents under the illumination by normally incident light. The currents of the two graphene valleys are mutually compensated providing zero net electric current. The magnitude and direction of the valley currents are determined by the parameters of strain and light polarization. For not too high photon energy strain-induced valley current exceeds that due to intrinsic warping of the graphene spectrum which suggests feasibility of strain-mediated valleytronics.

DOI: 10.1103/PhysRevB.90.075406 PACS number(s): 78.67.Wj, 72.80.Vp, 81.05.ue, 73.50.Pz

## I. INTRODUCTION

Although importance of the valley structure of the carrier spectrum in crystals has been recognized since the early age of solid-state physics, the idea to employ a valley degree of freedom as an internal characteristic independent of electric charge and spin was formulated only recently [1]. The related theoretical concepts and first successful experiments suggest an emergence of a direction called valleytronics. It assumes that in multivalley crystals nonzero currents in individual valleys can be generated keeping zero total electric current. In experiments, the valley control is realized with the use of carrier photoexcitation in a two-valley $MoS_2$ monolayer [2–4] and six-valley Si-based structure [5]. Moreover, valley Hall effect was observed recently for $MoS_2$ under the valley-selective optical excitation [6]. As a graphene band structure has two inequivalent valleys, this material is a potential candidate for development of valleytronics. Although no experimental indication of valley currents in graphene is present so far, various approaches of their generation as well as valley filtering were proposed. The activity was started by the papers [7,8] where the specific valley-dependent edge states of graphene nanoribbons are proposed to be used for the valley filtering. Another approach explores valley Hall effect in graphene with lifted sublattice equivalence [9–11]. After that, a number of various approaches were suggested [12–26]. One of them [23] employs warping of the graphene spectrum, which is essential at high carrier energies, above 1 eV. Such warping gives rise to valley currents under the optical excitation with light propagating normally to the graphene layer. It is important that anisotropy of the graphene energy spectrum can be not only due to its intrinsic properties (warping), but also under application of the external strain [27–29]. In this paper we analyze the valley currents of illuminated strained graphene. It is known that application of strain to graphene conserves the Dirac form of its spectrum, but leads to essential anisotropy of the Fermi velocity. Theoretical and experimental analysis suggest that such a behavior is sustained for strain magnitude as high as 10% [30–33]. According to our results, application of strain gives rise to greater photoinduced valley currents for midinfrared or softer illumination, compared to that due to natural warping. In addition, it allows external control of the valley currents in graphene structures with tunable strain parameters.

It is worth mentioning that other materials of the graphene family can also possess strain-induced spectrum asymmetry (see, for example, [34], where the spectrum of strained bigraphene was addressed), which suggests their perspectives for strain-controlled valleytronics.

## II. SPECTRUM OF GRAPHENE UNDER UNIFORM STRAIN

The honeycomb crystal lattice of unstrained graphene and the corresponding first Brillouin zone are shown in Figs. 1(a) and 1(b), respectively. The Brillouin zone extrema are at two inequivalent corners of the hexagon, $K$ and $K'$. The effect of the uniform strain on the energy spectrum of graphene was initially explored within the tight-binding approach and first-principles calculations [27,35–42]. The main results were that the opening of a gap in the energy spectrum requires very high values of strain, of the order of 20%. This means that the energy spectrum remains gapless and conelike for moderate uniform strains. However, the Dirac points in strained graphene no longer coincide with the edges of the Brillouin zone $K$ and $K'$. Moreover, the strong strain-induced anisotropy of Fermi velocity appears [27–29,35,37]. On the other hand, the properties of intrinsic graphene [43,44] and graphene subject to various fields [21,28,45–50], can be addressed based on the symmetry considerations. In particular, the $\mathbf{k}\cdot\mathbf{p}$ Hamiltonian $H$ of strained graphene can be developed [21,28,47] and has a form

$$\begin{aligned}
H &= H_k + H_\varepsilon + H_{\varepsilon k},\\
H_k &= \hbar v_F[(\hat{k}_x - i\hat{k}_y)\sigma_+ + (\hat{k}_x + i\hat{k}_y)\sigma_-],\\
H_\varepsilon &= E_{d1}\bar{\varepsilon} I + E_{d2}[(\varepsilon_\Delta + 2i\varepsilon_{xy})\sigma_+ + (\varepsilon_\Delta - 2i\varepsilon_{xy})\sigma_-],\\
H_{\varepsilon k} &= \hbar v_F\{a_2[(\hat{k}_x + i\hat{k}_y)(\varepsilon_\Delta + 2i\varepsilon_{xy})\\
&\quad + (\hat{k}_x - i\hat{k}_y)(\varepsilon_\Delta - 2i\varepsilon_{xy})]I + (2d_2 - 1)\bar{\varepsilon}[(\hat{k}_x - i\hat{k}_y)\sigma_+\\
&\quad + (\hat{k}_x + i\hat{k}_y)\sigma_-]/2 + (2g_2 - 1)[(\hat{k}_x + i\hat{k}_y)\\
&\quad \times (\varepsilon_\Delta - 2i\varepsilon_{xy})\sigma_+ + (\hat{k}_x - i\hat{k}_y)(\varepsilon_\Delta + 2i\varepsilon_{xy})\sigma_-]/2\},
\end{aligned} \tag{1}$$

*linnik1971@hotmail.com

 

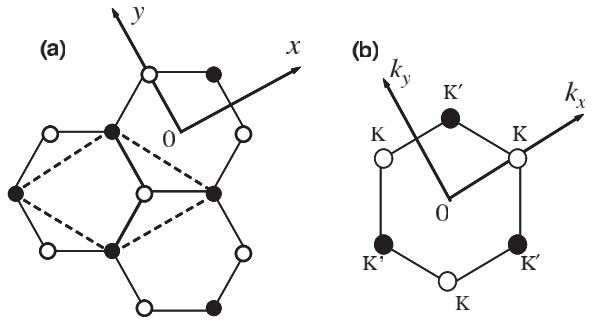


FIG. 1. (a) The honeycomb lattice of graphene. The carbon sites belonging to the two equivalent sublattices are denoted by solid and hollow circles. The dashed line marks the primitive cell. (b) The first Brillouin zone of graphene; the Dirac points of the graphene spectrum are at the $K$ and $K'$ valleys.

where Fermi velocity in unstrained graphene is $v_F = 10^6$ m/s, and $E_{d1}$ and $E_{d2}$ are the deformation potentials [51]. The coefficients $a_2 \approx 0.2$, $\tilde{d}_2 \approx -1.25$, and $\tilde{g}_2 \approx -2.14$ are responsible for the anisotropy of the Fermi velocity and were determined in [28] by the comparison with the first-principles calculations; $\sigma_\pm = \sigma_x \pm i\sigma_y$ are the combinations of Pauli matrices, $I$ is a $2 \times 2$ unity matrix, $k_\pm = k_x \pm ik_y$, and we introduce the uniaxial $\varepsilon_\Delta = \varepsilon_{xx} - \varepsilon_{yy}$, hydrostatic $\bar{\varepsilon} = \varepsilon_{xx} + \varepsilon_{yy}$, and shear $\varepsilon_{xy}$ components of strain.

It results in the Dirac-like electron and hole spectra $E_{\mathbf{k}}^{(c,v)}$ with anisotropic electron and hole Fermi velocities:

$$E_{\mathbf{k}}^{(c,v)} = \hbar[\pm v_0(\varphi) + \delta v(\varphi)]k. \tag{2}$$

Here $k$ and $\varphi$ are the absolute value and polar angle of momentum $\mathbf{k}$, $+$ and $-$ signs correspond to the conduction and valence bands, and we dropped the inessential for our problem strain-related momentum and energy shift of the Dirac point, the velocities are determined by

$$\begin{aligned} v_0(\varphi) &= v_F(1 + \bar{\varepsilon}\tilde{d}_2/2 + \varepsilon_\Delta \tilde{g}_2 \cos 2\varphi/2 + \varepsilon_{xy}\tilde{g}_2 \sin 2\varphi), \\ \delta v(\varphi) &= 2v_F a_2(\varepsilon_\Delta \cos\varphi - 2\varepsilon_{xy}\sin\varphi). \end{aligned} \tag{3}$$

As we see, the energy spectrum of strained graphene is essentially anisotropic and strain breaks not only the equivalence of $\mathbf{k}$ and $-\mathbf{k}$ directions but also the symmetry of electron and hole spectra as it is shown in Fig. 2. The corresponding solution for the wave function is

$$\begin{aligned} \Psi_k^{(c,v)}(\varphi) &= \frac{1}{\sqrt{2}} \begin{pmatrix} 1 \\ \pm C(\varphi) \end{pmatrix} e^{i\mathbf{k}\cdot\mathbf{r}}, \\ C(\varphi) &= e^{i\varphi} \frac{1 + \tilde{d}_2\bar{\varepsilon}/2 + \tilde{g}_2(\varepsilon_\Delta/2 + i\varepsilon_{xy})e^{-i2\varphi}}{\sqrt{1 + \tilde{d}_2\bar{\varepsilon} + \tilde{g}_2\varepsilon_\Delta \cos 2\varphi + 2\tilde{g}_2\varepsilon_{xy}\sin 2\varphi}}, \end{aligned} \tag{4}$$

where, as in (2), $+$ and $-$ signs mark the carrier bands. The provided spectra and wave functions are for the $K$ valley. For the $K'$ valley, the expressions for the spectrum and wave functions can be obtained by the substitution of $x \to -x$ for momentum and strain components, or, explicitly, $\varphi \to \pi - \varphi$ and $\varepsilon_{xy} \to -\varepsilon_{xy}$.

## III. LIGHT-INDUCED VALLEY CURRENTS

### A. Photogeneration valley currents

Before proceeding to rigorous analysis of the valley currents, let us discuss qualitatively its physical origin. In general, the valley current can appear due to anisotropy of the carrier group velocity and photon-induced transition probabilities. In Fig. 2 we plot the spectra of unstrained (red line) and strained (black line) graphene along the $k_y$ direction for the case of pure shear strain $\varepsilon_{xy}$. The vertical arrows show light-induced electron transitions from the valence to the conduction bands in the $K$ and $K'$ valleys. The arrows correspond to the $y$ components of the photogenerated electron and hole group velocities. As we see, in unstrained graphene the resulting current in each valley is exactly zero. In the presence of strain this is still true if the probabilities of transitions at positive and negative $k_y$ are equal. However, as we will see below, this is not the case (in the figure this is illustrated by the different vertical arrow thicknesses). As a result, each valley possesses nonzero current. These currents in the $K$ and $K'$ valleys are antiparallel, and there is no total current in the system.

The quantitative consideration of both effects can be done with the use of the steady state quasiclassical kinetic equation:

$$J^{(i)}\{f\} + J_R^{(i)}\{f\} + G^{(i)}\{f\} = 0, \tag{5}$$

where $f$ is the carrier distribution function, $J^{(i)}$ is the scattering integral, $J_R^{(i)}$ and $G^{(i)}$ are recombination and interband photogeneration rates, and index $i$ marks the valley. We concentrate on the case of moderate temperatures and excitation photon energy below the doubled intervalley (about 157 meV, zone-edge transverse optical phonon mode) energy [52]. In this case we can neglect the intervalley scattering, and the kinetic equations for each valley are decoupled. In the following we analyze a kinetic equation for the $K$ valley and drop the valley index for all values discussing the results for the $K'$ valley at the end of the section. We assume also that actual carrier energies are less than that of optical phonon (about 200 meV). Thus, we can also neglect the optical phonon scattering and take $J\{f\} = J_{\mathrm{LA}}\{f\} + J_{\mathrm{ee}}\{f\} + J_{\mathrm{im}}\{f\}$, considering scattering due to the longitudinal acoustic phonons (LA), impurity scattering (im), and electron-electron scattering (ee). Below we consider both intrinsic and doped graphene. However, we always assume that optical excitation generates carriers away from the Fermi energy level and we deal with a fully populated initial carrier state and empty finite state. Formally, this means that $G$ does not depend on the distribution function. In the presence of strain both wave functions and the light-electron interaction Hamiltonian [23] are modified, and we have

$$\begin{aligned} G = C_{\mathrm{eff}} \sum_{\mathbf{k}'} &\left|\left\langle \Psi_{\mathbf{k}'}^{(c)} \middle| (\sigma \cdot \mathbf{u} + \delta H_{\varepsilon u}) \middle| \Psi_{\mathbf{k}}^{(v)} \right\rangle\right|^2 \\ &\times \delta\left(E_{\mathbf{k}'}^{(c)} - E_{\mathbf{k}}^{(v)} - \hbar\omega\right), \quad C_{\mathrm{eff}} = 16\pi^2 v_F^2 \alpha I_o t^2/\omega^2, \end{aligned} \tag{6}$$

where $\sigma_i (i = x, y)$ are the Pauli matrices, $\alpha = e^2/4\pi\varepsilon_0\hbar c \approx 1/137$ is a dimensionless fine structure constant, and $I_0$, $\mathbf{u}$, and $\omega$ are the intensity, polarization, and the frequency of the incident light, respectively. We also introduce here the electric field amplitude transmission coefficient $t = 2/(n+1)$

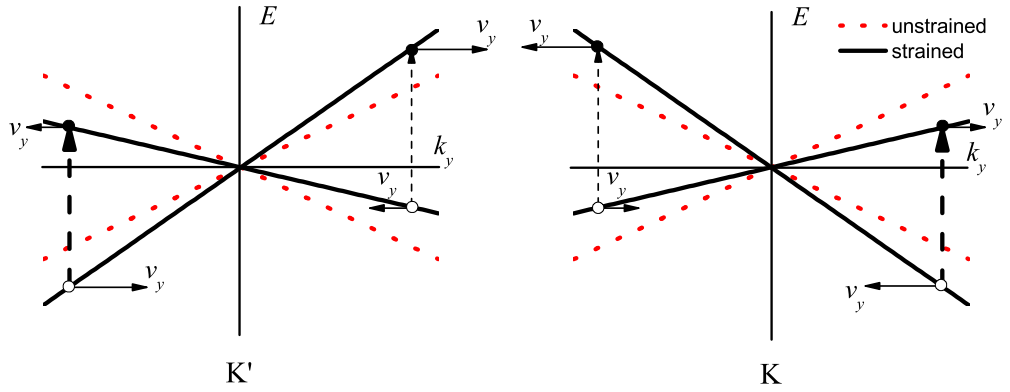


FIG. 2. (Color online) Comparison of the strained (solid line) with $\varepsilon_{xy} \neq 0$ and unstrained (dotted line) cross section of the graphene energy spectrum at $k_x = 0$. The light-induced transitions are marked by vertical arrows, with thicknesses reflecting the magnitude of the transition probability. The solid arrows of different lengths indicate the anisotropy of the group velocity.

assuming the graphene sheet is placed at the substrate with the refractive index $n$. $\Psi_{\mathbf{k}}^{(c,v)}$ are the wave functions of the conduction and valence bands which are determined by Eq. (4). The strain-induced contribution to the light-electron interaction $\delta H_{\varepsilon u}$ is analogous to the $H_{\varepsilon k}$ terms in the Hamiltonian of strained graphene given by Eq. (1) and is determined by the same constants:

$$\begin{aligned}\delta H_{\varepsilon u} = {} & a_2[(u_x + iu_y)(\varepsilon_\Delta + 2i\varepsilon_{xy}) \\ & + (u_x - iu_y)(\varepsilon_\Delta - 2i\varepsilon_{xy})]I + \tilde{d}_2\bar{\varepsilon}[(u_x - iu_y)\sigma_+ \\ & + (u_x + iu_y)\sigma_-]/2 + \tilde{g}_2[(u_x + iu_y)(\varepsilon_\Delta - 2i\varepsilon_{xy})\sigma_+ \\ & + (u_x - iu_y)(\varepsilon_\Delta + 2i\varepsilon_{xy})\sigma_-]/2. \end{aligned} \quad (7)$$

In the linear strain approximation $\delta H_{\varepsilon u}$ makes no contribution to the valley currents. Therefore, to avoid dealing with cumbersome expressions, we omit below the corresponding terms.

To solve Eq. (5) we use the standard approach [53], introducing as independent variables the distribution function energy $E$ and $\varphi$, and expanding $f$ into the Fourier series:

$$f(E,\varphi) = f_0(E) + \sum_{n=1}^{\infty}\left[f_n^{(c)}(E)\cos(n\varphi) + f_n^{(s)}(E)\sin(n\varphi)\right]. \quad (8)$$

In these variables the generation term is

$$\begin{aligned} G = {} & \mathrm{sgn}(E)\frac{C_{\mathrm{eff}}}{4}\left[1 + \left(u_y^2 - u_x^2\right)\cos(2\varphi) - 2u_xu_y\sin(2\varphi)\right] \\ & \times \delta\{|E|[1 - \mathrm{sgn}(E)\delta v(\varphi)/v_F] - \hbar\omega/2\}. \end{aligned} \quad (9)$$

In the following we assume that elastic scattering on various kinds of defects is the most efficient one. For the elastic scattering integral calculated assuming no strain effect on the carrier scattering probabilities $J_{\mathrm{im}}^{(0)}$, we have $J_{\mathrm{im}}^{(0)}\{f\} = -\sum_{n=1}^{\infty}[f_n^{(c)}(E)\cos(n\varphi) + f_n^{(s)}(E)\sin(n\varphi)]/\tau_n(E)$, where $\tau_n$ are determined by the elastic scattering probabilities [53]. Since $J_{\mathrm{im}}^{(0)}\{f\}$ contains no zero harmonic, $f_0$ is controlled by the other, less efficient, scattering mechanisms and we may assume that $f_0 \gg f_{n\neq 0}$.

Then, we introduce expansions $G = \sum_{n=0}^{\infty}[G_n^{(c)}(E)\cos(n\varphi) + G_n^{(s)}(E)\sin(n\varphi)]$, $J_\nu\{f_0\} = \sum_{n=0}^{\infty}[J_n^{(\nu,c)}(E)\cos(n\varphi) + J_n^{(\nu,s)}(E)\sin(n\varphi)]$, where $\nu$ marks the scattering mechanisms, including recombination. Note that for elastic scattering $J_{\mathrm{im}}\{f_0\} = 0$. As a result, for $f_{n\neq 0}$ we have an approximate equation

$$f_n^{(c,s)}(E) = \tau_n(E)\left[G_n^{(c,s)}(E) + \sum_\nu J_n^{[\nu,(c,s)]}(E)\right]. \quad (10)$$

Note that $J_n^{[\nu,(c,s)]}$ for $n \neq 0$ appears only due to strain-induced anisotropy. In the following we disregard this effect for the phonon, impurity, and electron-electron scattering. In general, it leads to the corresponding contributions of $f_n^{(c,s)}$ and, consequently, to the valley current. Those contributions are difficult to analyze quantitatively since they depend, in particular, on the microscopic details of the phonon scattering and peculiarities of many-electron effects under the electron-electron scattering. Thus, we assume

$$f_n^{(c,s)}(E) = \tau_n(E)\left[G_n^{(c,s)}(E) + J_n^{[R,(c,s)]}(E)\right], \quad (11)$$

and the corresponding valley current could be treated as a lower estimate.

Using the $E,\varphi$ variables, the expression for the valley current is

$$j_i = \frac{e}{2\pi^2\hbar^2}\int dE d\varphi \frac{E\,\mathrm{sgn}(E)v_i^{(g)}f(E,\varphi)}{v_E^2(\varphi)}, \quad i = x,y, \quad (12)$$

where $\mathbf{v}^{(g)} = \hbar^{-1}\nabla_k E$ is the carrier group velocity and $v_E(\varphi) = \mathrm{sgn}(E)v_0(\varphi) + \delta v(\varphi)$. According to (11), we can split the valley current into generation and recombination contributions $j_i^{(G)}$ and $j_i^{(R)}$ calculated by (12) for the corresponding contributions of the distribution functions $\tau_n(E)G_n^{(c,s)}(E)$ and $\tau_n(E)J_n^{[R,(c,s)]}(E)$. Since in our model $G$ does not depend on $f_0(E)$, it is straightforward to obtain explicit expression for $j_i^{(G)}$ which are valid for both intrinsic and doped graphene. This is not true for $j_i^{(R)}$. We postpone the related analysis of $f_0(E)$ and $j_i^{(R)}$ till the next section, concentrating here on the calculation of $j_i^{(G)}$.

The nonzero contribution to $j_i^{(G)}$ is provided by the zero harmonic of the factor $f(E,\varphi)v_i^{(g)}(E,\varphi)/v_E^2(\varphi)$. Restricting ourselves to the first-order contribution with respect to the magnitude of strain, we conclude that there are two inputs to

the valley current. The first one is due to $f_1^{(c,s)}$, which appears under the expansion of the $\delta$ function in (9). The second one is the first harmonic of $v_E^{-2}$. Both these contributions are stipulated by the strain-induced asymmetry of the electron and hole spectra, manifested in the anisotropy of the transition probability and effective density of states under the photon-induced transitions. As a result, we obtain for the electron part of $j_i^{(G)}$,

$$
\begin{aligned}
j_x^{(G)} &= \frac{\pi e a_2 \upsilon_F \alpha I_o t^2}{E_\omega^2}\Big\{\big[\varepsilon_\Delta\big(u_y^2-u_x^2\big)+2\varepsilon_\Delta+4\varepsilon_{xy}u_xu_y\big]\frac{d}{dE}\{E^2\tau_1(E)\}|_{E=E_\omega} \\
&\quad + 2E_\omega\tau_2(E_\omega)\big[\varepsilon_\Delta\big(u_y^2-u_x^2\big)+4\varepsilon_{xy}u_xu_y\big]\Big\}, \\
j_y^{(G)} &= \frac{2\pi e a_2 \upsilon_F \alpha I_o t^2}{E_\omega^2}\Big\{\big[\varepsilon_{xy}\big(u_y^2-u_x^2\big)-2\varepsilon_{xy}-\varepsilon_\Delta u_xu_y\big]\frac{d}{dE}\{E^2\tau_1(E)\}|_{E=E_\omega} \\
&\quad + 2E_\omega\tau_2(E_\omega)\big[\varepsilon_{xy}\big(u_y^2-u_x^2\big)-\varepsilon_\Delta u_xu_y\big]\Big\},
\end{aligned}
\tag{13}
$$

where $E_\omega = \hbar\omega/2$. For the hole part, we have analogous expressions but with the minus sign and substitution $E_\omega \to -E_\omega$. To obtain the expression for the photocurrent in the $K'$ valley we must change the sign of all $x$ components for all vectors ($\mathbf{j}^{(G)}$ and $\mathbf{u}$) and $\varepsilon_{xy}$. This means that the partial valley currents of the two valleys have opposite signs being equal in magnitude, which results in a zero net electric current in accordance with the symmetry arguments.

Let us proceed with some quantitative estimates. First of all, it is worth comparing the strain-induced valley current and that due to natural warping of the graphene spectrum [23]. To be specific, we assume elastic scattering by the unscreened Coulomb impurities in intrinsic graphene, where $\tau_1 \sim E$ and $\tau_2 = 3\tau_1$ [23]. Taking parameters of warping from [23], for light polarized along the $y$ direction and $\varepsilon_{xy} = 0$, the ratio of the warping $j_x^{(w)}$ and strain-induced valley currents is

$$
\frac{j_x^{(w)}}{j_x^{(G)}} = \frac{1}{96 a_2 \varepsilon_\Delta}\frac{\hbar\omega}{E^*}, \tag{14}
$$

where $E^* \approx 17.5$ eV denotes the energy where characteristic warping and Dirac contributions to the spectrum are comparable [23]. Thus, for realistic strain $\varepsilon_\Delta = 1\%$ strain-induced valley current exceeds the warping one for $\hbar\omega < 1$ eV. This means that for long-wavelength radiation, starting from the midinfrared band, it is feasible to deal with strain-controlled valley current. Taking $\hbar\omega = 0.4$ eV and $\tau_{1\omega} = 10^{-14}$ s [54], for the provided above strain, light intensity $I_0 = 10^2$ W/m$^2$ and the substrate refractive index $n = 2.6$, corresponding to SiC we estimate $j_x{}^{(G)} = 2\times 10^{-3}$ pA/$\mu m$.

### B. Recombination-induced valley currents

In analogy to the above considered photogenerated valley currents the strain-induced anisotropy of the energy spectrum leads also to the appearance of the valley currents due to the inverse recombination processes. In general, a number of recombination processes are possible in graphene, including radiative, phonon-assisted, and Auger process [55]. For the considered excitation energy optical-phonon-assisted recombination is suppressed, while the Auger recombination is inefficient (see [56]). Thus, we concentrate on the former mechanism where spontaneous and thermal radiation-induced interband transitions take place. To estimate this effect we use the collision integral for the thermal radiation interband transitions given in Ref. [57]. So, for positive energies corresponding to the conduction band, an explicit expression for $J_R$ is

$$
\begin{aligned}
J_R\{f(E,\varphi)\} &= \nu_E^{(R)}\{N_{\rm ph}(E,\varphi)[1-f(E,\varphi)]f(E',\varphi) \\
&\quad - [N_{\rm ph}(E,\varphi)+1][1-f(E',\varphi)]f(E,\varphi)\}, \\
\nu_E^{(R)} &= \frac{\upsilon_r}{\hbar\upsilon_F}E\left[1-\delta\upsilon(\varphi)/\upsilon_F\right], \\
E' &= -E + 2E\delta\upsilon(\varphi)/\upsilon_F,
\end{aligned}
\tag{15}
$$

and for negative energies, corresponding to the valence band, $J_R$ can be written in an analogous way. Here $N_{\rm ph}(E,\varphi) = (\exp\{2E\left[1-\delta\upsilon(\varphi)/\upsilon_F\right]/T\}-1)^{-1}$ is the Plank distribution function, $T$ is temperature in energy units, and $\upsilon_r = 8\alpha n \upsilon_F\,(\upsilon_F/c)^2/3$ is the characteristic radiative velocity.

As we mentioned above, to analyze the recombination current, we need to determine the isotropic component of the distribution function $f_0(E)$. Restricting ourselves to the linear in strain magnitude contributions to the valley current, we should address this problem assuming no presence of strain. Even in this case this is a complicated problem, requiring, in general, extensive numerical simulations. Below we consider two limiting cases, which allow an approximate solution: the cases of intrinsic and heavily doped graphene.

#### *1. Intrinsic graphene*

At low temperatures the concentration of carriers of the intrinsic graphene is small and as a result one can neglect the carrier-carrier interaction. This case was thoroughly analyzed in [57]. The distribution function at low pumping is split as $f_0(E) = f^{(\rm eq)}(E) + {\rm sgn}(E)\Delta f(|E|)$, where $f^{(\rm eq)}(E) = [\exp(E/T)+1]^{-1}$ is the equilibrium distribution and the small nonequilibrium correction $\Delta f(E)$ is determined by the interplay between the thermal radiation generation-recombination processes and the quasielastic energy relaxation due to the acoustic phonon scattering.

After some algebra for the first order in strain contribution to the recombination scattering integral we obtain

$$J_R\{f_0\} = \frac{\upsilon_r}{\hbar\upsilon_F^2}\delta\upsilon(\varphi)E\frac{d}{dE}\left[\frac{E\Delta f(E)}{\sinh(E/T)}\right], \quad (16)$$

which provides the following expression for the recombination valley current:

$$\begin{Bmatrix} j_x^{(R)} \\ j_y^{(R)} \end{Bmatrix} = \frac{e}{\pi^2\hbar^3}\frac{\upsilon_r a_2}{\upsilon_F^2}\begin{Bmatrix} -\varepsilon_\Delta \\ 2\varepsilon_{xy} \end{Bmatrix} \times \int_0^\infty dE\frac{E\Delta f(E)}{\sinh(E/T)}\frac{d}{dE}[E^2\tau_1(E)]. \quad (17)$$

Naturally, if carrier relaxation due to acoustic phonon scattering is weak, $\Delta f$ is concentrated near $E = E_\omega$ and the absolute value of the recombination current is of the same order as generation one, leading to its partial compensation. However, this is typically not the case [57], and $\Delta f(E)$ is localized in the region $E \sim T$. To analyze the importance of the recombination current we have to take into account that particle conservation under the generation-recombination process requires that $\int_0^\infty dE E^2\Delta f(E)\sinh^{-1}(E/T) = \text{const}$ [57]. For elastic scattering by the unscreened Coulomb impurities $\tau_1 \sim E$. Therefore, presence of the extra energy power in the expression for the recombination valley current with respect to the normalization integral suggests that it is considerably less than the generation one. For example, for the same parameters used under calculation of the generation current and $T = 50$ K we obtain that the recombination valley current is directed opposite to generation one, and its absolute value $j^{(R)} \sim 10^{-5}$ pA/$\mu$m is about two orders of magnitude smaller than $j^{(G)}$. Here we take the same parameters characterizing acoustic phonon scattering as that used in [57,58], namely, the deformation potential constant $D = 12$ eV, density $\rho_S = 7.6 \times 10^{-7}$ kg/m$^{-2}$, and sound velocity $s = 7.3 \times 10^3$ m/s.

### 2. Doped graphene

Another case which allows explicit estimate of the recombination valley current is the case of doped graphene. For high enough carrier concentration electron-electron interaction is more efficient than phonon scattering. On the other hand, electron-electron scattering can still be less efficient than elastic scattering by impurities. So, for the Fermi energy $E_F = 34$ meV, which corresponds at low temperatures to the electron concentration $n_e = 10^{15}$ m$^{-2}$, the charged impurity scattering time can be estimated as $\tau_2 = 5 \times 10^{-14}$ s [54]. For electrons at the chosen excitation energy the electron-electron scattering time is of the order of 0.3–0.1 ps and is much shorter than the acoustic-phonon scattering times of the order of 5–1 ps [59]. For this relaxation times hierarchy it is reasonable to assume that $f_0(E)$ is close to the Fermi distribution function but with temperature $T_e$ higher than the lattice and photon temperature $T$ due to the light-induced heating of the electron gas. Naturally, at equilibrium with $\Delta T = T_e - T = 0$, the recombination valley current is zero, and for low excitation power we expect it to be proportional to the ratio $\Delta T/T$. It should be determined from the energy balance which equates the energy input rate due to optical excitation and energy relaxation rate, which in our case is due to acoustic phonon scattering. Note that in the following we disregard the light-induced variation of $E_F$ since for weak excitation power it provides no contribution to the valley current. As in the previous subsection, the distribution function splits as $f_0(E) = f^{(\text{eq})}(E) + \Delta f(E)$, where $f^{(\text{eq})}(E) = \{\exp[(E - E_F)/T] + 1\}^{-1}$ is the equilibrium distribution and the small nonequilibrium correction $\Delta f(E) = \frac{\partial f^{(\text{eq})}}{\partial T}\Delta T$. For high enough doping with $E_F/T \gg 1$ we obtain the following expressions for the recombination-induced valley current components:

$$\begin{Bmatrix} j_x^{(R)} \\ j_y^{(R)} \end{Bmatrix} \cong \frac{216}{\pi}\frac{e\upsilon_r a_2 T^4}{\hbar^3\upsilon_F^2}\begin{Bmatrix} -\varepsilon_\Delta \\ 2\varepsilon_{xy} \end{Bmatrix}\frac{\tau_{1\omega}}{E_\omega}\frac{\Delta T}{T}e^{-E_F/T}. \quad (18)$$

As we mentioned above, the light-induced heating $\Delta T$ is determined from the energy balance equation:

$$\int E^2[J_{\text{LA}}\{f_0(E)\} + J_R\{f_0(E)\} + G]\,dE d\varphi = 0. \quad (19)$$

Using the explicit form of the collision integral $J_{\text{LA}}$ [57]:

$$J_{\text{LA}}\{f_0(E)\} = \left(\frac{s}{\upsilon_F}\right)^2\frac{\upsilon_{\text{ac}}}{\hbar\upsilon_F T}\frac{1}{E}\frac{d}{dE}\left[E^4\frac{df^{(\text{eq})}(E)}{dE}\right]\Delta T, \quad (20)$$

we arrive at the following expression for the light-induced heating:

$$\frac{\Delta T}{T} = \frac{\alpha\pi^2(\hbar\upsilon_F)^3 I_0 t^2}{2E_F^4\upsilon_{\text{ac}}}\left(\frac{\upsilon_F}{s}\right)^2, \quad (21)$$

where $\upsilon_{\text{ac}} = D^2T/(4\hbar^2\rho_S\upsilon_F s^2)$ is the characteristic acoustic-phonon scattering velocity. The contribution of recombination to the energy balance is negligibly small and the corresponding term is omitted in Eq. (21). Note that in some actual setups lattice and photon temperatures could be different and this changes the energy balance conditions [60]. Finally, using Eqs. (18) and (21) we obtain an expression for the ratio of the recombination and generation-induced valley currents:

$$j^{(R)}/j^{(G)} \approx \frac{36}{5}\frac{\upsilon_r}{\upsilon_{\text{ac}}}\left(\frac{\upsilon_F}{s}\right)^2\left(\frac{T}{E_F}\right)^4 e^{-E_F/T}. \quad (22)$$

For the above chosen parameters we have $\upsilon_{\text{ac}} = 1424$ m/s, $\upsilon_r = 0.34$ m/s, $\Delta T/T \sim 0.02$, and the current ratio is $j^{(R)}/j^{(G)} \sim 10^{-6}$. So one can make the conclusion that the recombination-induced valley currents in doped graphene are negligibly small compared to the generation ones.

## IV. CONCLUSIONS

To conclude, we analyzed the appearance of the valley current in strained graphene under monochromatic optical excitation. The valley current is possible due to the strain-induced electron-hole spectrum anisotropy. Under midinfrared and softer irradiation for realistic strain magnitudes the considered mechanism of the valley current generation is considerably more efficient than that related to the warping

natural graphene spectrum, proposed previously. It is shown that the reverse process of carrier recombination is inessential for valley current formation for both intrinsic and doped graphene due to efficient carrier energy relaxation. The feasible valley current magnitude is about $10^{-3}$ pA/$\mu$m and potentially it can be governed in strain-controlled structures.


## ACKNOWLEDGMENTS

The author thanks V. A. Kochelap for stimulating discussions and acknowledges the hospitality of the Abdus Salam International Centre for Theoretical Physics (Trieste), where this work was completed. This work was supported by the STCU Project No. 5716.



[1] S. A. Tarasenko and E. L. Ivchenko, JETP Lett. **81**, 231 (2005).
[2] G. Sallen, L. Bouet, X. Marie, G. Wang, C. R. Zhu, W. P. Han, Y. Lu, P. H. Tan, T. Amand, B. L. Liu, and B. Urbaszek, Phys. Rev. B **86**, 081301(R) (2012).
[3] H. Zeng, J. Dai, W. Yao, D. Xiao, and X. Cui, Nat. Nanotech. **7**, 490 (2012).
[4] K. F. Mak, K. He, J. Shan, and T. F. Heinz, Nat. Nanotech. **7**, 494 (2012).
[5] J. Karch, S. A. Tarasenko, E. L. Ivchenko, J. Kamann, P. Olbrich, M. Utz, Z. D. Kvon, and S. D. Ganichev, Phys. Rev. B **83**, 121312(R) (2011).
[6] K. F. Mak, K. L. McGill, J. Park, and P. L. McEuen, Science **344**, 1489 (2014).
[7] L. Brey and H. A. Fertig, Phys. Rev. B **73**, 235411 (2006).
[8] A. Rycerz, J. Tworzydlo, and C. W. J. Beenakker, Nat. Phys. **3**, 172 (2007).
[9] D. Xiao, W. Yao, and Q. Niu, Phys. Rev. Lett. **99**, 236809 (2007).
[10] M. Koshino and T. Ando, Phys. Rev. B **81**, 195431 (2010).
[11] M. Koshino, Phys. Rev. B **84**, 125427 (2011).
[12] J. L. Garcia-Pomar, A. Cortijo, and M. Nieto-Vesperinas, Phys. Rev. Lett. **100**, 236801 (2008).
[13] A. S. Moskalenko and J. Berakdar, Phys. Rev. B **80**, 193407 (2009).
[14] D. S. L. Abergel and T. Chakraborty, Appl. Phys. Lett. **95**, 062107 (2009).
[15] J. M. Pereira, F. M. Peeters, R. N. Costa Filho, and G. A. Farias, J. Phys.: Condens. Matter. **21**, 045301 (2009).
[16] A. Chaves, L. Covaci, Kh. Yu. Rakhimov, G. A. Farias, and F. M. Peeters, Phys. Rev. B **82**, 205430 (2010).
[17] T. Nakanishi, M. Koshino, and T. Ando, Phys. Rev. B **82**, 125428 (2010).
[18] T. Fujita, M. B. A. Jalil, and S. G. Tan, Appl. Phys. Lett. **97**, 043508 (2010).
[19] F. Zhai, X. Zhao, K. Chang, and H. Q. Xu, Phys. Rev. B **82**, 115442 (2010).
[20] D. Gunlycke and C. T. White, Phys. Rev. Let. **106**, 136806 (2011).
[21] Z. G. Zhu and J. Berakdar, Phys. Rev. B **84**, 195460 (2011).
[22] Z. Wu, F. Zhai, F. M. Peeters, H. Q. Xu, and K. Chang, Phys. Rev. Lett. **106**, 176802 (2011).
[23] L. E. Golub, S. A. Tarasenko, M. V. Entin, and L. I. Magarill, Phys. Rev. B **84**, 195408 (2011).
[24] F. Zhai and K. Chang, Phys. Rev. B **85**, 155415 (2012).
[25] Z. Niu, J. Appl. Phys. **111**, 103712 (2012).
[26] Y. Jiang, T. Low, K. Chang, M. I. Katsnelson, and F. Guinea, Phys. Rev. Lett. **110**, 046601 (2013).
[27] S. M. Choi, S. H. Jhi, and Y. W. Son, Phys. Rev B **81**, 081407(R) (2010).
[28] T. L. Linnik, J. Phys.: Condens. Matter **24**, 205302 (2012).
[29] F. de Juan, M. Sturla, and M. A. H. Vozmediano, Phys. Rev. Let. **108**, 227205 (2012).
[30] C. Lee, X. Wei, J. W. Kysar, and J. Hone, Science **321**, 385 (2008).
[31] I. W. Frank, D. M. Tanenbaum, A. M. van der Zande, and P. L. McEuen, J. Vac. Sci. Technol. B **25**, 2558 (2007).
[32] Z. H. Ni, T. Yu, Y. H. Lu, Y. Y. Wang, Y. P. Feng, and Z. X. Shen, ACS Nano **2**, 2301 (2008).
[33] K. S. Kim, Y. Zhao, H. Jang, S. Y. Lee, J. M. Kim, K. S. Kim, J.-H. Ahn, P. Kim, J.-Y. Choi, and B. H. Hong, Nature (London) **457**, 706 (2009).
[34] V. G. Litovchenko, A. I. Kurchak, and M. V. Strikha, Ukr. J. Phys. **59**, 79 (2014).
[35] V. M. Pereira, A. H. Castro Neto, and N. M. R. Peres, Phys. Rev. B **80**, 045401 (2009).
[36] C. Yang, W. Shaofeng, and X. Hong, Eur. Phys. J. Appl. Phys. **52**, 20601 (2010).
[37] M. O. Goerbig, J.-N. Fuchs, G. Montambaux, and F. Piechon, Phys. Rev. B **78**, 045415 (2008).
[38] R. M. Ribeiro, V. M. Pereira, N. M. R. Peres, P. R. Briddon, and A. H. Castro Neto, New. J. Phys. **11**, 115002 (2009).
[39] G. Cocco, E. Cadelano, and L. Colombo, Phys. Rev. B **81**, 241412 (2010).
[40] M. Mohr, K. Papagelis, J. Maultzsch, and C. Thomsen, Phys. Rev. B **80**, 205410 (2009).
[41] V. M. Pereira, R. M. Ribeiro, N. M. R. Peres, and A. H. Castro Neto, Europhys. Lett. **92**, 67001 (2010).
[42] Y. Li, X. Jiang, Z. Liu, and Z. Liu, Nano Res. **3**, 545 (2010).
[43] W. M. Lomer, Proc. R. Soc. London Ser. A **227**, 330 (1955).
[44] J. C. Slonczewski and P. R. Weiss, Phys. Rev. **109**, 272 (1958).
[45] J. L. Manes, Phys. Rev. B **76**, 045430 (2007).
[46] D. M. Basko, Phys. Rev. B **78**, 125418 (2008).
[47] R. Winkler and U. Zulicke, Phys. Rev. B **82**, 245313 (2010).
[48] J. L. Manes, F. de Juan, M. Sturla, and M. A. H. Vozmediano, Phys. Rev. B **88**, 155405 (2013).
[49] D. C. Cabra, N. E. Grandi, G. A. Silva, and M. B. Sturla, Phys. Rev. B **88**, 045126 (2013).
[50] F. de Juan, Phys. Rev. B **87**, 125419 (2013).
[51] T. Ando, J. Phys. Soc. Jpn. **74**, 777 (2005).
[52] R. Kim, V. Perebeinos, and P. Avouris, Phys. Rev. B **84**, 075449 (2011); F. Rana, P. A. George, J. H. Strait, J. Dawlaty, S. Shivaraman, M. Chandrashekhar, and M. G. Spencer, *ibid.* **79**, 115447 (2009).
[53] F. T. Vasko and O. E. Raichev, *Quantum Kinetic Theory and Applications* (Springer, New York, 2005).

[54] S. Das Sarma, S. Adam, E. H. Hwang, and E. Rossi, Rev. Mod. Phys. **83**, 407 (2011).
[55] F. Rana, Phys. Rev. B **76**, 155431 (2007).
[56] F. T. Vasko and V. V. Mitin, Phys. Rev. B **84**, 155445 (2011).
[57] F. T. Vasko and V. Ryzhii, Phys. Rev. B **77**, 195433 (2008).
[58] A. Satou, F. T. Vasko, and V. Ryzhii, Phys. Rev. B **78**, 115431 (2008).
[59] Qiuzi Li and S. Das Sarma, Phys. Rev. B **87**, 085406 (2013).
[60] P. N. Romanets, F. T. Vasko, and M. V. Strikha, Phys. Rev. B **79**, 033406 (2009).